Materials Science and Engineering A 527 (2010) 5575–5581

Contents lists available at ScienceDirect

Materials Science and Engineering A

journal homepage: www.elsevier.com/locate/msea

Impact properties of tempered bainite–ferrite dual phase steels

N. Saeidi*, A. Ekrami

Department of Materials Science and Engineering, Sharif University of Technology, Tehran, Iran

ARTICLE INFO

Article history:
Received 26 October 2009
Received in revised form 1 May 2010
Accepted 10 May 2010

Keywords:
Dual phase steel
Charpy impact energy
Tempered bainite–ferrite

ABSTRACT

To improve both strength and toughness of AISI 4340 steel three microstructures, full bainite, bainite–ferrite and tempered bainite–ferrite, were produced by heat treatment of this steel. Tensile, impact and hardness properties of these microstructures were compared. The results showed that with tempering of bainite–34% ferrite dual phase steel, elongation and charpy impact energy increased significantly in comparison to bainite and bainite–ferrite microstructures. Also ductile-brittle transition temperatures of bainite–ferrite and tempered bainite–ferrite steels were measured and confirmed superior toughness properties of this microstructure. Fracture surface analysis of charpy specimens also showed increase in toughness of tempered bainite–ferrite in comparison to bainite–ferrite and full bainite microstructures. Radial marks, shear lip areas and crack initiation site region in fracture surfaces of three mentioned microstructures were also considered and compared.

1. Introduction

AISI/SAE 4340 steel have many applications in the aircraft, aerospace, automobile and nuclear power industries. In these applications strength and resistance to fracture are important parameters.

High strain rate deformations and impact properties of this steel have been analyzed in some previous works [1,2,3]. Lee and co-workers showed that 4340 steel is tougher in dynamic rather than static loading. Also they showed that tempering of this steel at 350 °C causes tempered martensite embitterment of steel [3].

Also many works have done to improve both strength and toughness, such as use of tempered martensite microstructure [4] or for better toughness, lower bainite [5]. One of the best microstructure which gives both good strength and toughness is dual phase microstructure. In this field Tomita and co-workers have done a lot of investigation on martensite-bainite dual phase 4340 steel. They found that tempered martensite with 0.25 volume fraction of bainite provide a better combination of strength and ductility than tempered martensite or bainite microstructures [6,7]. It has been also reported that lower bainite is tougher than tempered martensite in AISI 4340 steel [4]. Since ferrite is tougher than lower bainite, it is expected that bainite–ferrite dual phase steels show better toughness than lower bainite.

Khakian found that in bainite–ferrite dual phase 4340 steel, elongation will increase with increase of ferrite volume fraction up to 34% but with more increase in ferrite volume fraction elongation will decrease [8]. It seems that this microstructure has the optimum toughness properties. The present research were undertaken to consider impact properties of ferrite-bainite dual phase steel with 34% volume fraction of ferrite, and impact fracture surfaces were also studied.

2. Materials and methods

AIS14340 steel bars with chemical composition given in Table 1 were used in this study.

The steel was received in the form of 30 mm diameter bars. Tensile and charpy V-notched specimens were cut from the bars and semifinished by machining, prior to heat treatment. The specimens then homogenised at 1000 °C for 2 h and then heat treated according to Table 2 heat treatment cycles.

For each microstructure three charpy impact test specimens and for BFT microstructure three tensile specimens were also prepared. After prescribed heat treatments, all specimens were ground to final dimensions. The charpy impact specimens were prepared according to ASTM E23 standard [9], and impact tests were carried out at different temperatures to determine ductile–brittle transition temperature. For obtaining high temperatures, boiling water was used and subzero temperatures were obtained by mixture of water, NaCl and methanol. Thermal conditioning during this process was done according to ASTM E23. That is for thermal conditioning the sequence of removing the test specimen from its cooling (or heating) medium with centering tongs (which temperature conditioned with the test specimen), placing the specimen in the test position and releasing the pendulum in less than 5 s (for standard $10 \times 10 \times 55$ mm specimens).

* Corresponding author. Fax: +98 21 67005717.
E-mail address: navidsae@gmail.com (N. Saeidi).

0921-5093/$ – see front matter © 2010 Elsevier B.V. All rights reserved.
doi:10.1016/j.msea.2010.05.015

Table 1
Chemical composition of used AISI 4340 steel.

Element	C	Si	Mn	P	S	Cr	Ni	Mo	Fe
%Wt	0.40	0.29	0.62	0.019	0.004	0.73	1.77	0.21	Balance

Table 2
The used heat treatment cycles.

	Microstructure	Heat treatment
(I)	Full bainite (B)	Austenitizing at 850 °C (60 min), austempering at 300 °C (60 min), air cooling.
(II)	Bainite–34% ferrite (BF)	Austenitizing at 850 °C (60 min), isothermal transformation at 700 °C (100 min), austempering at 300 °C (60 min), air cooling.
(III)	Tempered bainite–34% ferrite (BFT)	As II and then tempered at 250 °C (120 min), air cooled.

Ductile fracture percentage of broken specimens was determined according to ASTM E23 [9]. To do this, the appearance of the fracture surfaces of the specimens were compared with fracture appearance chart showed in Annex A6 of ASTM E23 [9].

The tensile specimens were prepared according to ASTM-A370 [10] and tested with an Instron tensile machine with a cross head speed of 2 mm/min.

The hardness values were determined using a Rockwell C indenter with an applied load of 150 kg.

Metallographic studies were done on samples prepared and etched by solution regent consisted of 16 g $Na_2S_2O_3$, 5 g $K_2S_2O_5$ and 100 ml distilled water. Ferrite volume fraction was measured by "Image J" image analyzer software [11]. More information about using this software can be obtained from Ref. [12].

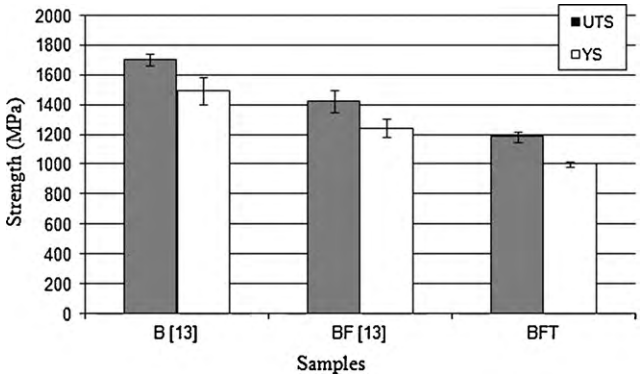

Fig. 2. Strength of B, BF and BFT steels.

3. Results and discussion

Optical micrographs of produced microstructures are shown in Fig. 1. Image analysis showed about 34% ferrite in the BF microstructure.

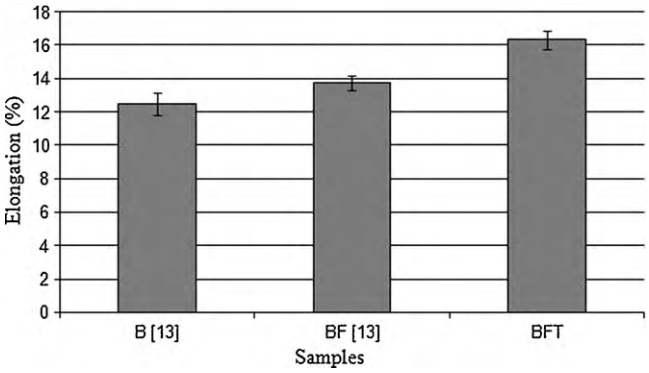

Fig. 3. Elongation %.

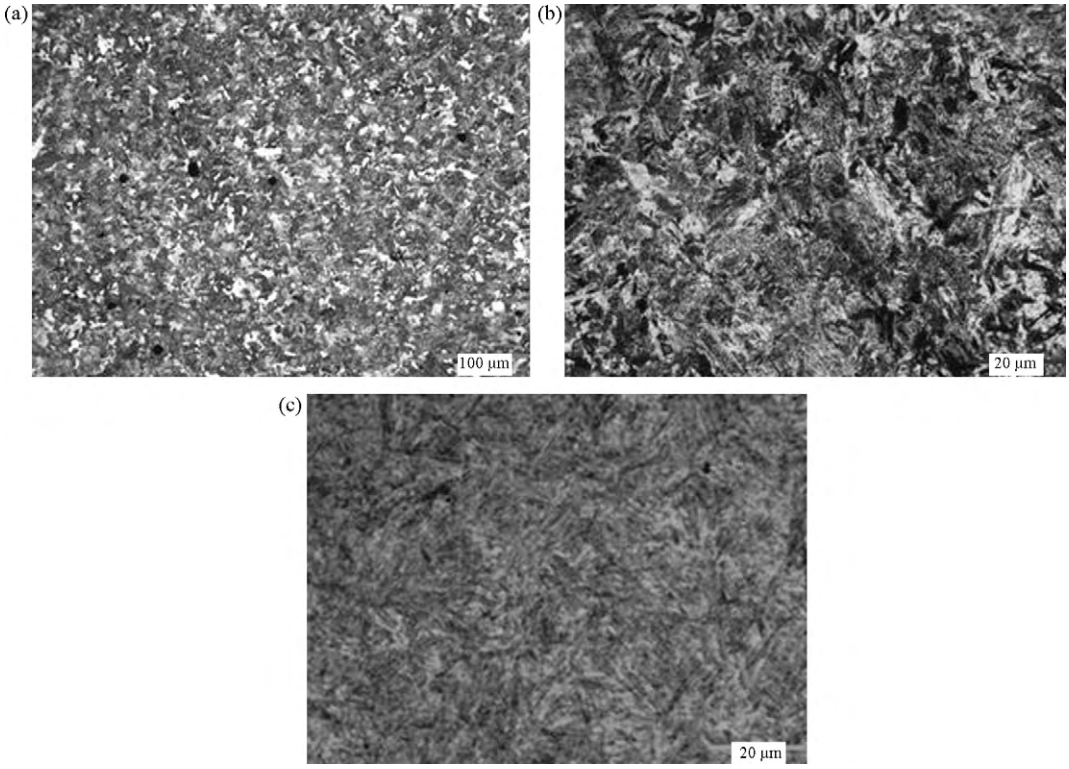

Fig. 1. Microstructures of (a) BF and (b) BFT and (c) B steels.

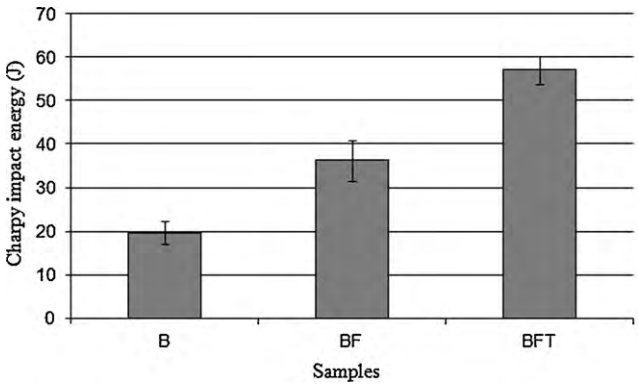

Fig. 4. Averaged impact energy of B, BF and BFT steels, at room temperature.

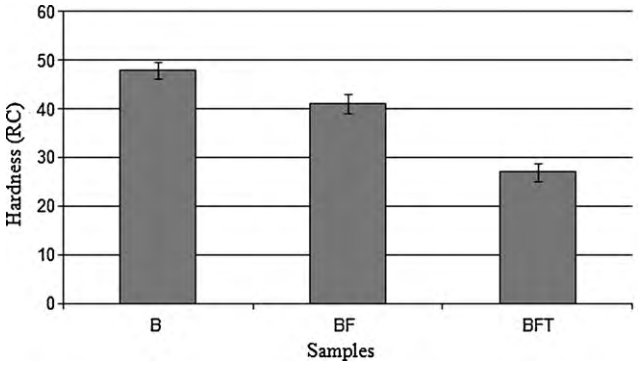

Fig. 5. Hardness of B, BF and BFT steels.

The room temperature mechanical properties of B, BF and BFT steels are shown in Figs. 2–5. Tensile properties of B and BF steels were taken from the previous paper [13].

As can be seen from Figs. 2 and 3 by changing bainite microstructure to bainite–34% ferrite, the ultimate strength and yield strength decreased about 250 and 280 Mpa respectively and elongation increased about 1.3%. With tempering of BF steel, the strength decreases (Fig. 2) but its elongation increases about 2.6% and 3.9% in comparison to BF and B steels respectively (Fig. 3). Increase of

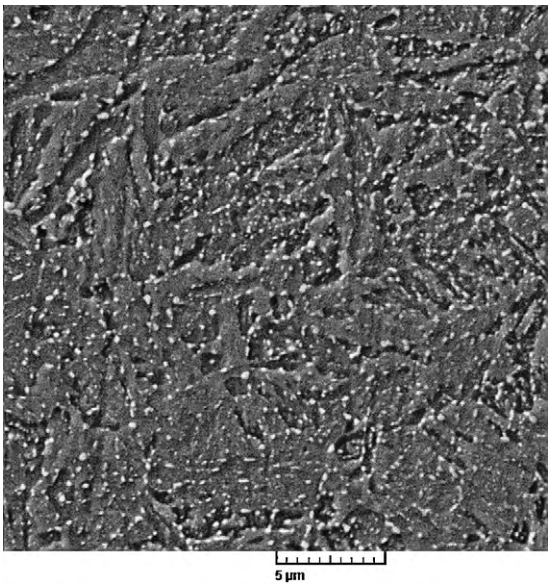

Fig. 6. SEM micrograph of BFT steel.

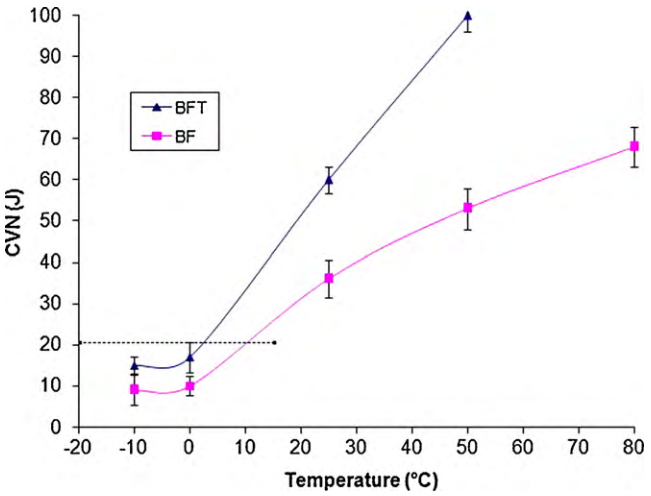

Fig. 7. Charpy impact energy versus temperature.

elongation in BF, in comparison to B steel, can be attributed to the presence of soft and ductile ferrite phase in the vicinity of bainite [13].

Higher impact energy of BF steel (Fig. 4), in comparison to B steel, can be related to increase of dislocation density at the front of crack tip and blunting of crack tip [5,6,14]. According to the investigation of Akbarpour and Ekrami [5], dual phase ferrite-bainite steel strain hardened in two stages, at the first stage only ferrite deforms plastically and at the second stage both ferrite and bainite deform plastically. Therefore it is expected that dislocation density of ferrite be more than that in bainite. It is also reported [14] that with increasing dislocation density at the front of crack tip, its radius will increase and material shows more toughness than single phase state.

According to Fig. 6, BFT microstructure, fine globular carbide particles dispersed homogenously within the microstructure. Tempering is a term historically associated with heating the martensite at a given temperature and involves many different basic processes, such as: precipitation of carbides, decomposition of retained austenite, and recovery and recrystallisation of martensite structure [15].

Mechanical properties of BFT microstructure can be discussed as the tempered martensite. But there are some differences. For example, due to the high formation temperature of bainite, auto-tempering process is unavoidable and redistribution of carbon

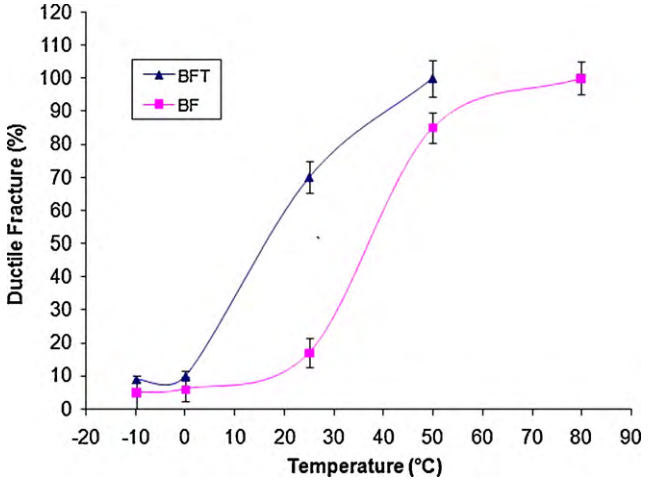

Fig. 8. Ductile fracture percent versus temperature.

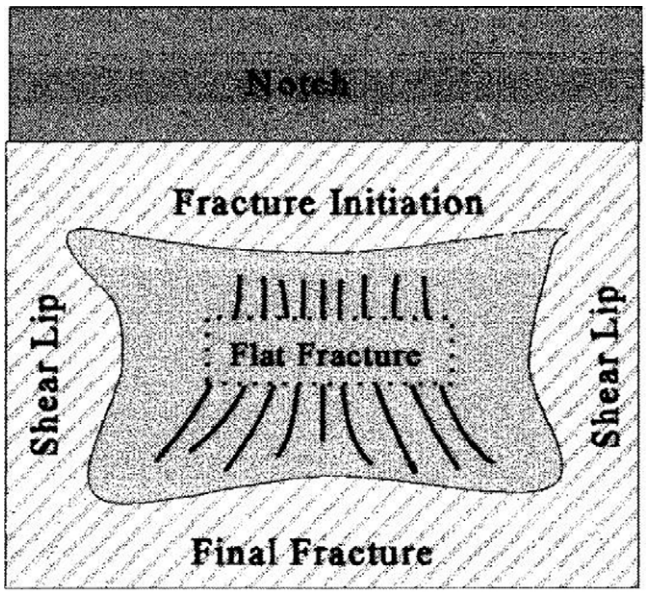

Fig. 9. Schematic illustration of charpy fracture surface [9].

from saturated ferrite into remaining austenite and precipitation of carbide during bainite formation occurs rapidly [16]. On the other hand, during intercritical annealing in the austenite–ferrite two phase region, the amount of carbon in austenite increases, because of low solubility of carbon in ferrite. Therefore bainite produced during austempering process, would have more carbon content. Therefore it is expected that carbide particles already exist in bainite and tempering causes coarsening of these particles like overaging process, so reduction of strength and hardness is expected (Figs. 2 and 5). According to Fig. 5 with tempering of BF at 250 °C for 2 h the hardness decreases about 50%. Also it has been reported that rapid decrease of hardness is due to the change of ferrite plates into equiaxed shape [17].

Figs. 7 and 8 show charpy impact energy and variation of ductile fracture percentage with temperature for BF and BFT steels respectively. The ductile–brittle transition temperatures (DBTT) from the test data are determined based on the criterion of 20.4 J (15 ft-lb) absorbed energy [14]. It is about 10 °C for BF and 2 °C for BFT steel (Fig. 7). This means, impact resistance of BF dual phase steels increases with tempering.

According to ASTM E23 [9] charpy fracture surface can be shown as Fig. 9. It is seen that fracture surface consists of four regions. Crack initiation site just blow the notch, shear lip region near the edges of the specimen, final fracture region on the opposite of the notch and in the center there is flat fracture with the appearance of radial mark which point to the crack initiation site or crack root region.

Figs. 10–12 show fracture surface of charpy impact BF and BFT steels tested at 0 °C. It can be seen that the radial marks point to the origin of the fracture (Fig. 10). Crack initiation site consists of dimples as shown in Fig. 11. It can be seen from Fig. 10 that crack initiation site in BFT steel is wider and have larger and deeper dimples than BF steel (Fig. 11). The existence of wider low crack extension area (in the crack initiation site region) in the BFT steel means that the crack extension rate in the BFT steel is lower than that in BF steel and this can contribute to the higher impact energy of BFT steel.

Fig. 12 shows SEM micrograph of radial mark region of fracture surface shown in Fig. 10. It can be seen that a mixed fracture mechanism, consist of cleavage and ductile, exist together. This type of fracture is called quasi cleavage fracture.

Fig. 13 shows fracture surface of BF and BFT charpy specimens tested at 25 °C. It is seen that radial marks point to the origin of the crack and shear lips area and crack initiation site are wider than those in steels tested at 0 °C (Fig. 10). However, these areas for BFT microstructure are still larger than those in BF which confirms the higher impact energy of BFT steel (Fig. 7).

Fig. 14 shows SEM micrographs of crack root of fracture surfaces shown in Fig. 13. It is seen that the crack root consists of dimples which are larger than that at 0 °C. Fig. 15 shows SEM micrograph of radial mark regions of charpy impact fracture surfaces at 25 °C. It can be seen that at this temperature fracture mechanism is quasi cleavage while its dimples and cleavage facets are finer than those observed at 0 °C.

The appearance of the radial marks is partially dependent on ductility of the material. When ductility is high, radial marks are finer [17] such as seen in Figs. 10 and 13. For steels tested at high temperatures (BF at 80 °C and BFT at 50 °C) these radial marks can not be seen but contour shape lines that move away from the crack initiation site, is observable (Fig. 16). There are also large and curved shear lips indicate the ductile fracture of BF and BFT steels tested at these temperatures.

According to the obtained results it can be concluded that with producing of dual phase with BF microstructure, charpy impact energy and elongation increase. With tempering of this microstructure and producing BFT microstructure, these properties increase more but strength and hardness considerably decrease in comparison to bainite microstructure. Fractography of fracture surfaces of charpy impact test samples also showed improvement of toughness properties. It was observed that with increasing of charpy impact energy and elongation, shear lip and crack initiation site

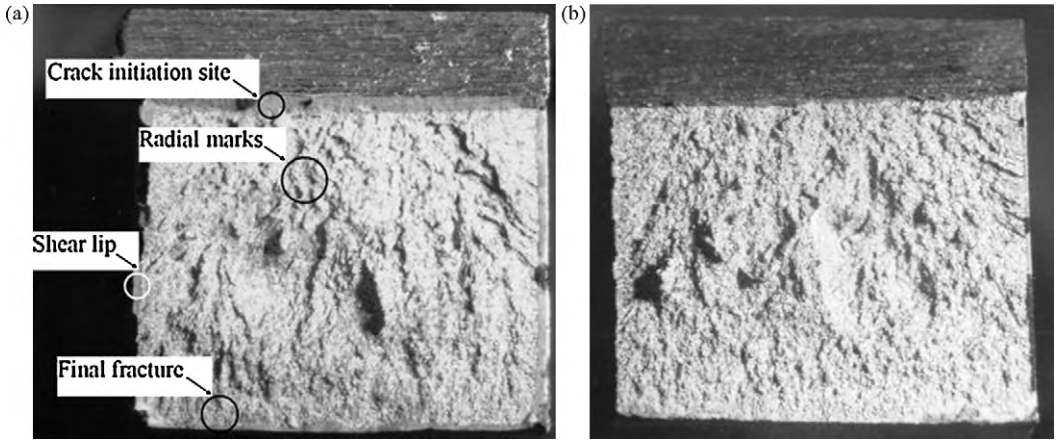

Fig. 10. Stereo microscope micrographs of charpy impact surface of (a) BFT and (b) BF steel at 0 °C.

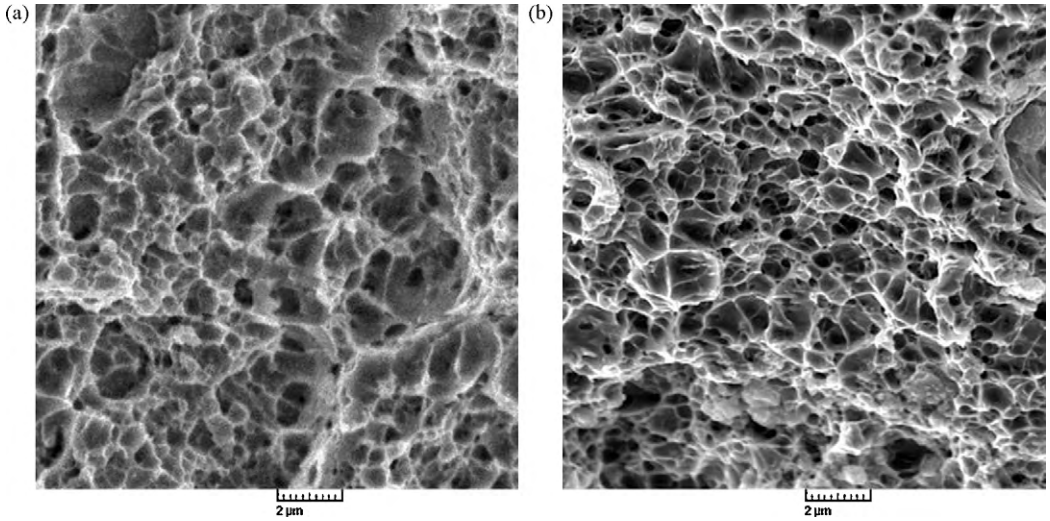

Fig. 11. SEM micrographs of crack initiation site at fracture surface of (a) BFT and (b) BF steel.

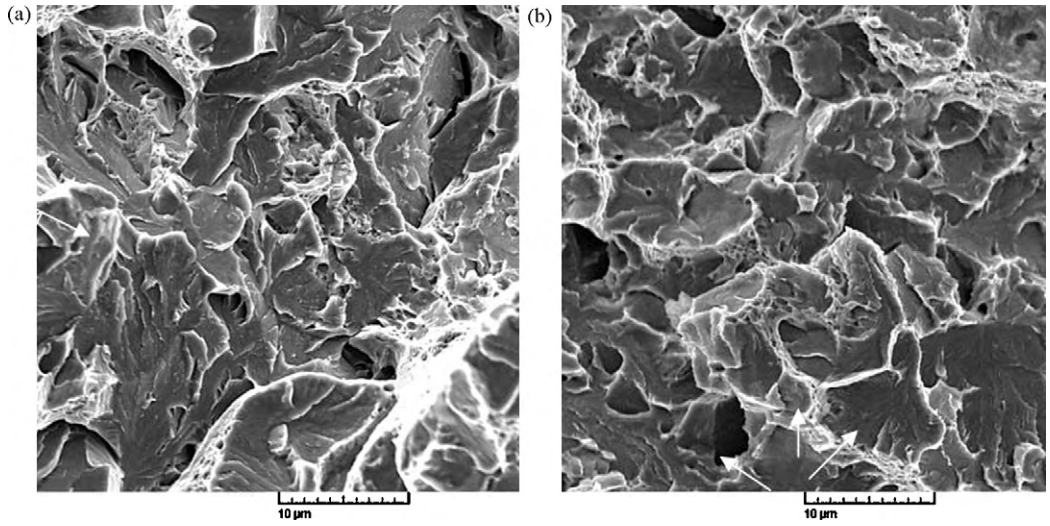

Fig. 12. SEM micrographs of central region of charpy impact surface of (a) BFT and (b) BF steel.

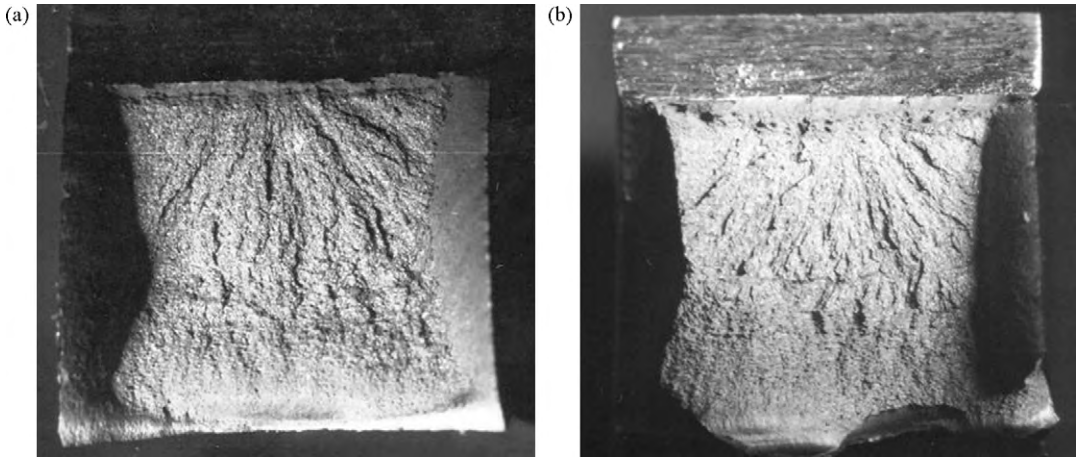

Fig. 13. Fracture surfaces of (a) BF and (b) BFT charpy specimen, tested at 25 °C.

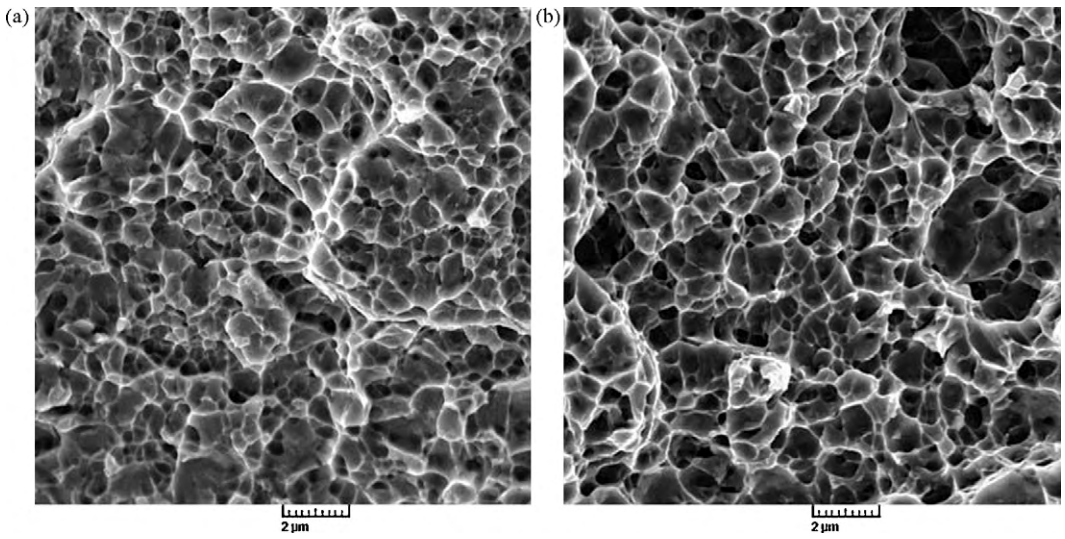

Fig. 14. SEM micrographs of notch root of charpy impact (a) BF (b) BFT specimen, tested at 25 °C.

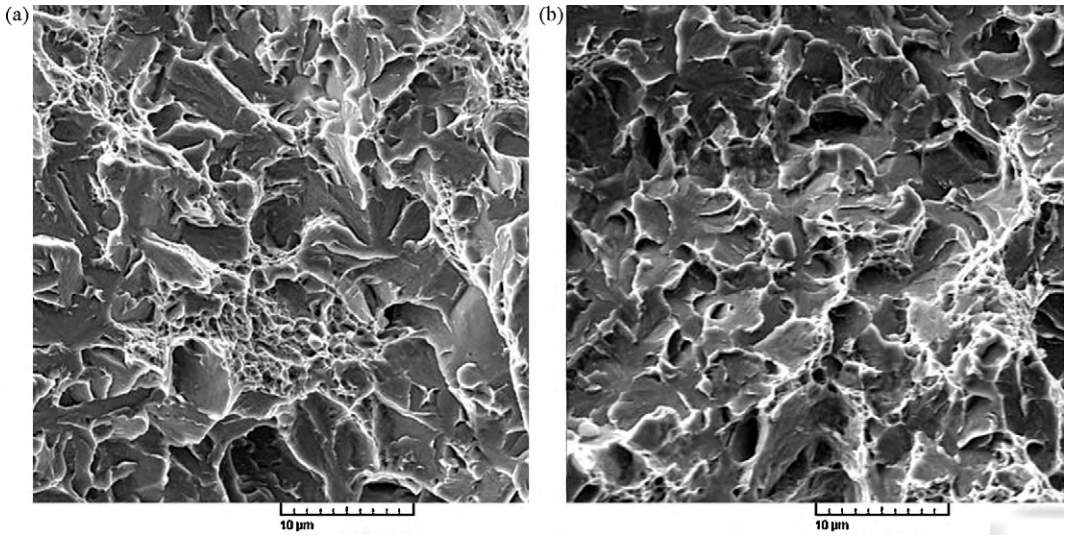

Fig. 15. SEM micrographs of radial mark region (a) BF (b) BFT specimen, tested at 25 °C.

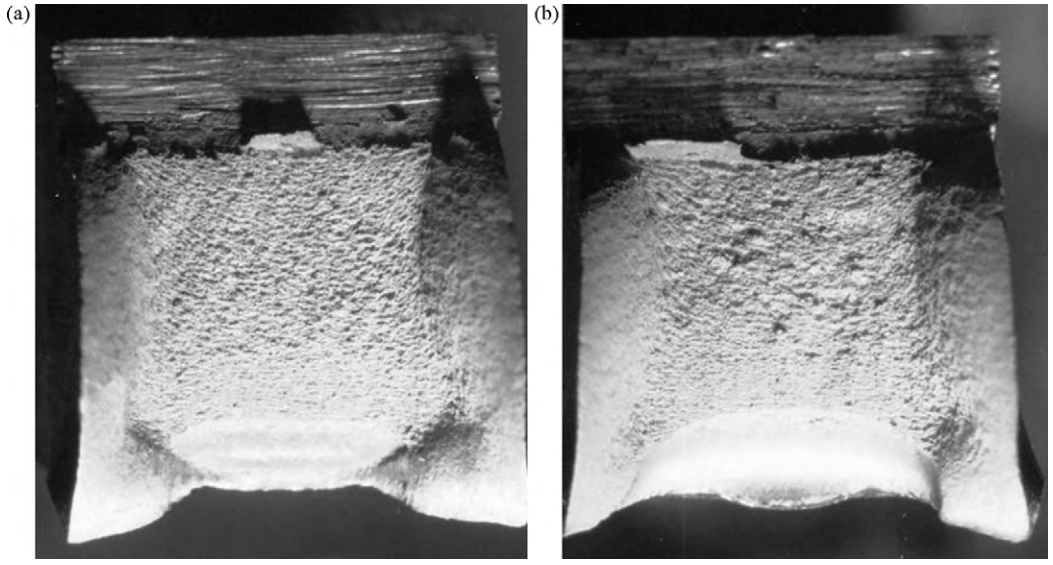

Fig. 16. Charpy impact fracture surface of (a) BF at 80 °C and (b) BFT steel, tested at 50 °C.

areas increase and radial marks change to the finer shapes which confirm better toughness of BFT steel.

4. Conclusion

From the result of mechanical and microscopic studies of B, BF and BFT microstructures, the following can be drawn:

Between B, BF and BFT microstructures, BFT microstructure showed the highest charpy impact energy at room temperature.

In spite of low difference in hardness between B and BF microstructure, BF microstructure showed about 50% more charpy impact energy. But BFT microstructure showed less hardness and more charpy impact energy than BF microstructure.

Tempering of BF microstructure caused decrease of ultimate strength and yield strength, which is related to carbide particle coarsening.

Fracture surface observations confirmed variation of impact energy. Radial marks in fracture surface tend to be finer and shear lip areas tend to increase, with increase in charpy impact energy or changing the microstructure from B to BF and BFT. Also it was observed that with increase in test temperature, the area of crack initiation site region increased.

References

[1] W.S. Lee, H.F. Lam, Journal De Physique. IV 4 (1994) 307–312.
[2] G.E. Gazza, F.R. Larson, American Society for Metals-Transactions 58 (1965) 183–194.
[3] Y.C. Chi, S. Lee, K. Cho, J. Duffy, Materials Science and Engineering A 114 (1989) 105–126.
[4] J.M. Tartaglia, K.A. Lazzari, G.P. Hui, K.L. Hayrynen, Metallurgical and Materials Transactions A 39A (2008) 559.
[5] M.R. Akbarpour, A. Ekrami, Materials Science and Engineering A 477 (1–2) (2008) 306–310.
[6] Y. Tomita, K. Okabayashi, Metallurgical Transactions 14A (1983) 485–492.
[7] Y. Tomita, Metallurgical Transactions 18A (1987) 1495–1501.
[8] M. Khakian, MSc thesis, Sharif University of technology, Tehran Iran, 2006.
[9] Annual book of ASTM Standards, E23, 2001.
[10] Annual book of ASTM Standards, A370, 2001.
[11] C.E. Campbell, J.C. Zhaob, M.F. Henry, Materials Science and Engineering A 407 (2005) 135–146.
[12] http://rsb.info.nih.gov/ij/.
[13] N. Saeidi, A. Ekrami, Materials Science and Engineering A 523 (2009) 125–129.
[14] R.W. Hertzberg, Deformation and Fracture Mechanics of Engineering Materials, 4th Ed., Wiley, USA, 1996.
[15] W.S. Lee, T.T. Su, Journal of Materials Processing Technology 87 (1999) 198–206.
[16] H.K.D.H. Bhadeshia, “Bainite in Steels”, Second Edition, 2001.
[17] ASM Handbook, Vol. 12, PP. 200, 1996.